Geological Magazine

Supporting Information for

Miocene to sub-Recent magmatism at the intersection between the Dead Sea Transform and the Ash Shaam volcanic field, evidence from the Yarmouk River gorge and vicinity

Amit Segev[1*], Itay J. Reznik[1], Uri Schattner[2]

[1]Geological Survey of Israel, 32 Yeshayahu Leibowitz st., Jerusalem 9692100, Israel

[2]Dr. Moses Strauss Department of Marine Geosciences, Leon H. Charney School of Marine Sciences, University of Haifa, Mt. Carmel, Haifa 31905, Israel

*Corresponding author: Amit Segev (amit.segev@gsi.gov.il)

Contents of this file

- Data and reliability of various geochronological sources and methods
- Figures SM1-SM12

Data and reliability of various geochronological sources and methods

The study area is part of a long-lasting (~26 Myr) prolific volcanic field, rich with basic magmatic bodies. These bodies recorded the geomagnetic polarity during their formation, and given the frequent reversals, the abundant basaltic units form a complete magneto-stratigraphy succession (SM1). The location, age, and polarity of the magmatic bodies are comparable to the 1-km grid Reduced-To-Pole magnetic anomaly map (Schattner et al., 2019). Hence, the exact timing of the magmatism is crucial to interpreting the magnetic anomalies and understanding the regional tectono-magmatic setting.

Basaltic rocks from the Galilee and the Golan were K–Ar measured by the Geological Survey of Israel (GSI) geochronological laboratory since ~1980 (Mor and Steinitz, 1985). Considerable improvements in measurement precision during the eighties produced more accurate dates for the Cover Basalt Formation (Mor et al., 1990) and the Lower Basalt Formation (Shaliv, 1991). Still, interpretations of K–Ar measurements presented broad date ranges of magmatic/volcanic activity mainly due to analytical problems. Thus, the actual duration of volcanic events remained uncertain. When the $^{40}Ar/^{39}Ar$ step-heating (plateau ages) dating analyses were applied on some of the samples (Heimann et al., 1996), the original K–Ar date ranges were significantly narrowed and constrained. These differences stress the high uncertainty of the K–Ar method. Usually, the $^{40}Ar/^{39}Ar$ total gas date is suffering similar problems as the K–Ar method because it does not detect Ar loss, recoil or deficit, and excess Ar in the sample. The significant difference in age between these methods appeared in Heimann (1990).

The K–Ar age determinations of rocks from Zemah-1 well were carried out by Steinitz and Lang (1984 a, b) in the GSI laboratory. Their report was published in Appendix 3, in Marcus et al. (1984). The data of Steinitz and Lang (1984 a, b) was re-evaluated by Segev (2017; Fig. SM2), who concluded that the date determination was influenced by clastic grains contamination within the light fraction of the magmatic rocks. These grains are most likely of Precambrian date, as demonstrated by the sample from 3,281-3,287 m depth that yielded a date of 547 ±17 Ma. Therefore, most of the whole rock (WR) samples yielded mixed K–Ar dates that are too high. However, some of the magnetic separates yielded relatively low dates than the Ar-Ar total gas dating (see below), but within their analytical error. In general, the low-resolution K–Ar dates of the magnetic separates from rocks in Zemah-1 well delivered a fairly good age estimation (Fig. SM2).

Recent studies established reliable $^{40}Ar/^{39}Ar$ plateau ages for the Neogene volcanic sequence in the Lower Galilee (Rozenbaum et al. 2016). These ages are used here as stratigraphic markers for the new interpretation herein. Only sporadic $^{40}Ar/^{39}Ar$ ages were published to date for Zemah-1 Well. These include the plateau age of olivine micro gabbro at a depth of 2674 m (4.05±0.07 Ma, Heimann et al., 1996), and two additional total gas dates that were published by Stein (2014) based on unpublished data from Heimann (Fig. SM2).

Additional $^{40}Ar/^{39}Ar$ plateau and total gas ages and K–Ar dates were obtained mainly for the northern DST segment, between the Kinneret and Hula basins (Heimann, 1990). The Yarmouk Basalt from Naharayim (Yarmouk-Jordan Rivers confluence), close to Zemah-1 Well, is $^{40}Ar/^{39}Ar$, dated to 0.66±0.09 Ma (Plateau; Heimann and Braun, 2000). Inbar and Gilichinsky (2009), Weinstein et al. (2013) and Behar et al. (2019) dated the latest volcanic eruptions in several sites on the Golan using $^{40}Ar/^{39}Ar$ plateau. They obtained ages of 1,000-600 ka for the early phase and 120-95 ka for the latest volcanic phase.

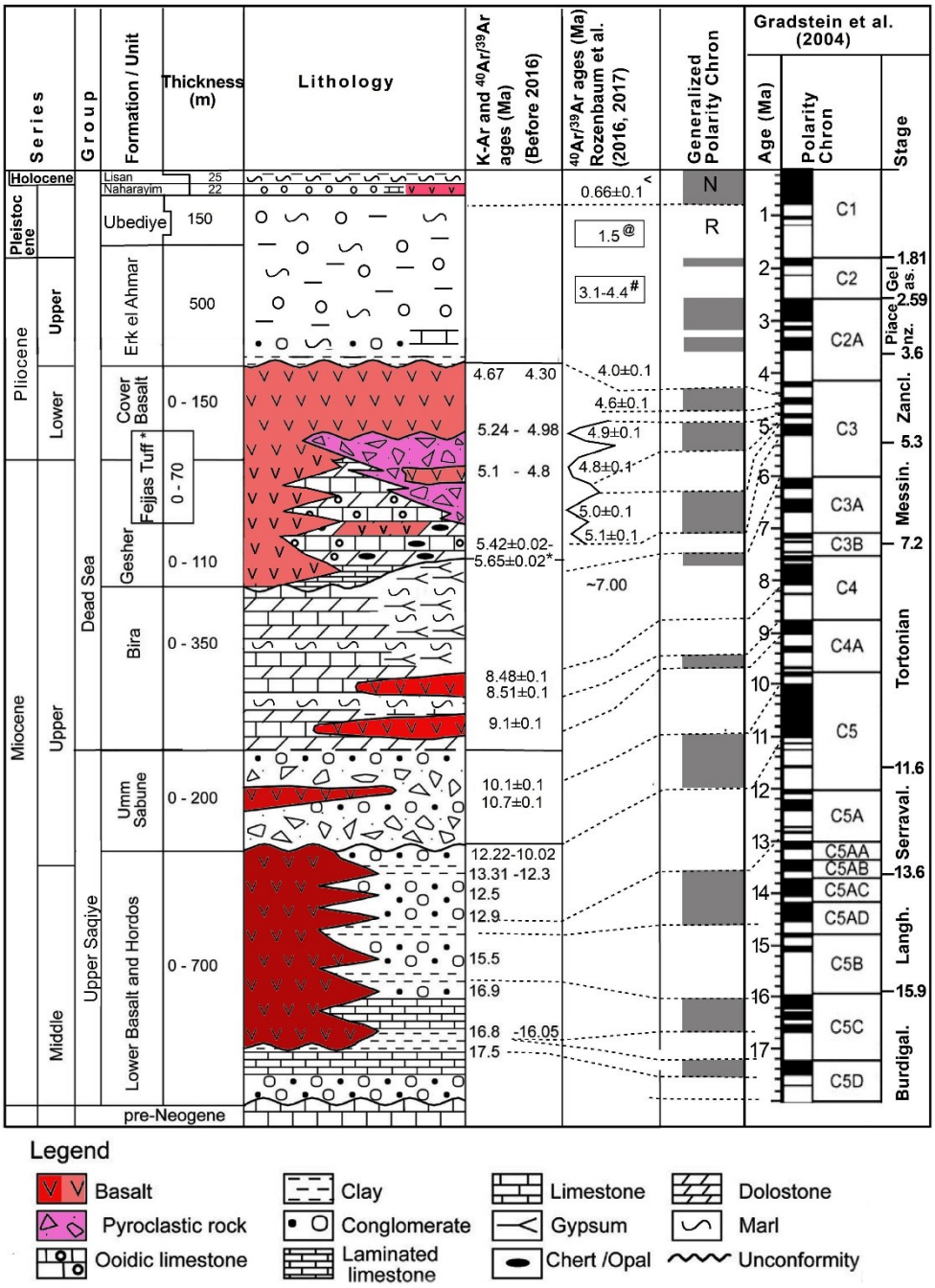

Figure. SM1 - Litho-, chrono- and magneto- stratigraphy of the southeastern Lower Galilee since the Miocene (modified after Rozenbaun et al., 2016; earlier radiometric ages are from Shaliv, 1991; Heimann et al., 1996; Segev, 2000). Polarity chrons and time scale after Gradstein et al. (2004). Volcanic units are emphasized in red colors.

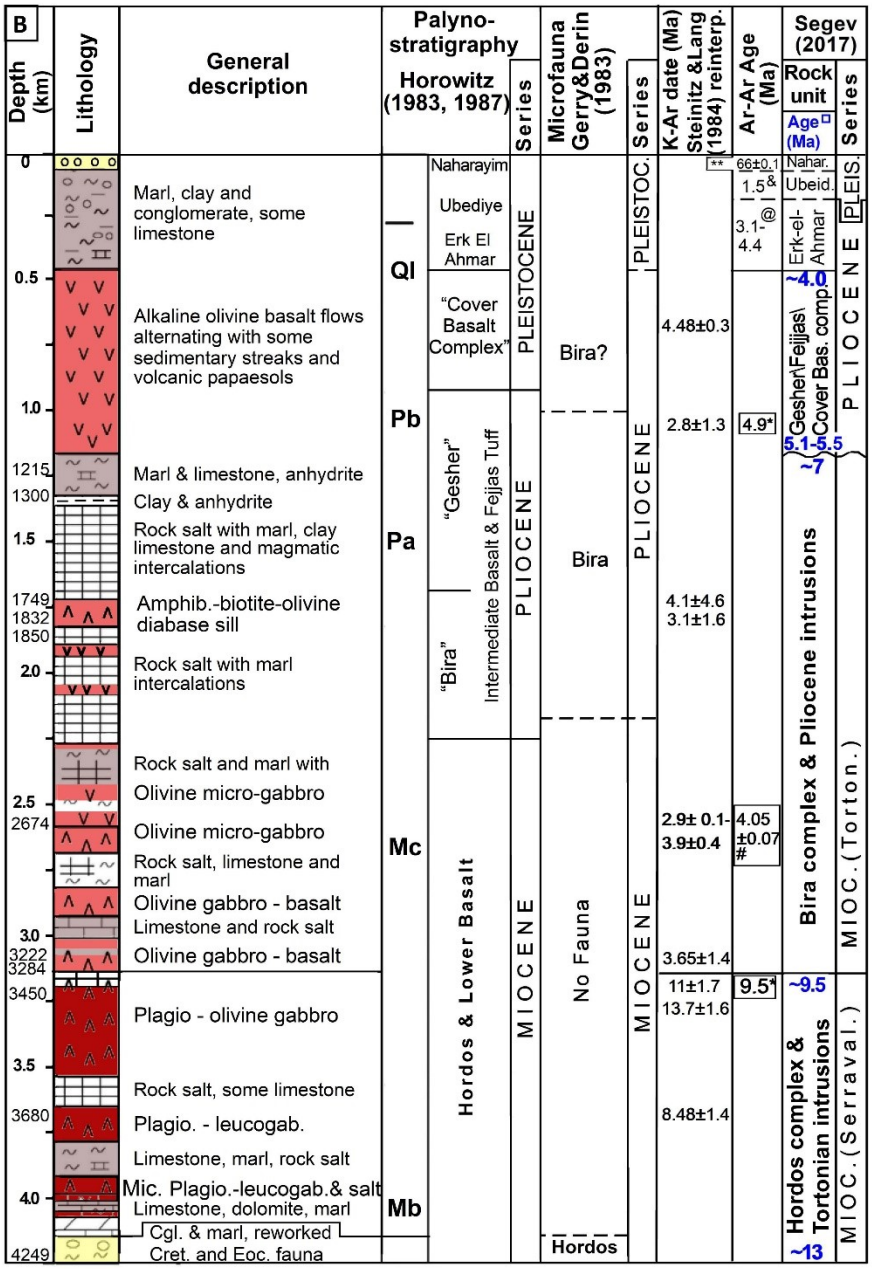

Figure SM2 - Stratigraphic correlation and compilation of radiometric ages from Zemah-1 Well. The simplified lithology is modified after Marcus & Slager (1985) and Sandler et al. (2001). Markings: # Heimann et al. (1996); * Heimann & Stein, in Stein (2014); ** Heimann & Braun (2000); @ Cosmogenic burial dating (Davis et al., 2011); & Dating hominid remains, tools and fauna (Martinez-Navarro et al., 2009; Tchernov, 1987). M - Miocene, P - Pliocene, Q - Quaternary. Ql - Pleistocene oriental spruce forest wet, warm temp; Pb - Late Pliocene spruce and oak park forest dry, cool temp; Pa - Early-Middle Pliocene spruce and oak forest wet, cool temp; Mc - Late Miocene compositae and Chenopodiaceae dry, hot desert; Mb - Mid Miocene Lowland damp Forest wet, subtropical.

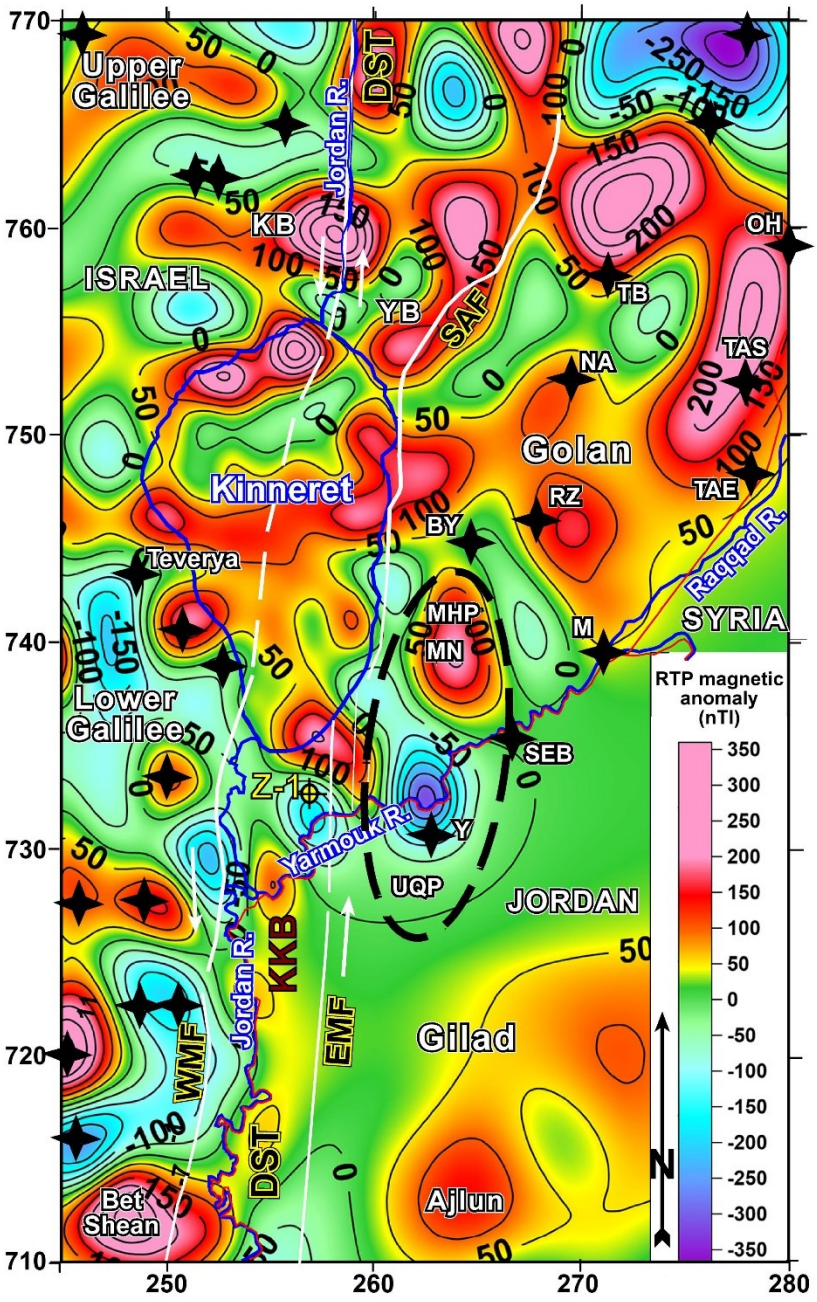

Figure SM3 – Reduced-To-Pole (RTP) magnetic anomaly map of the study area (after Schattner et al., 2019 and therein explanations). Black stars mark previously mapped volcanic centers. Thick black dashed ellipse marks the suggested extent of the Yarmouk Cover Basalt volcano. DST – Dead Sea Transform, KB – Korazim Block, NA – Natur, RZ – Rugum Zaki, YB – Yhudiya-Beteikha, BY – Bnei Yehuda, MHP – Mevo Hama Plateau, UQP – Umm Qays Plateau, MN – Mt. Nimron, Z-1 – Zemah-1 Well, EMF – Eastern Marginal Fault, WMF – Western Marginal Fault. Basalt/scoria eruptive centers marked: TB – Tel Bezek, TAS – Tel A-Saki, TAE – Tel Abu Eitar, K – Koayiah volcano, M – Meitzar volcano, SEB – Shaq el Barid volcano, Y – Yarmouk volcano. Israel Transverse Mercator (ITM) coordinates divided by 1,000.

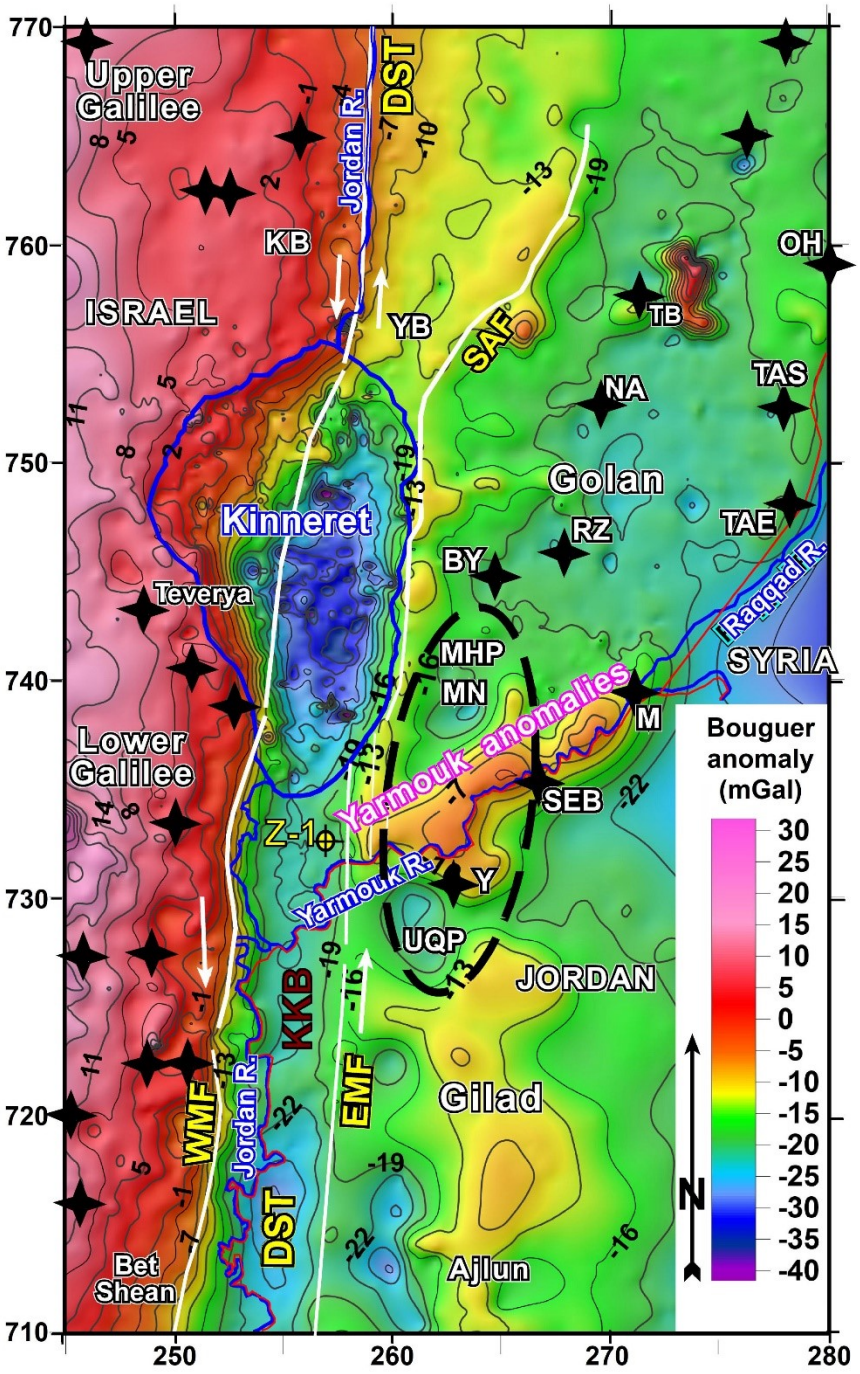

Figure SM4 – Bouguer gravity anomaly map of the study area (data from Rosenthal et al., 2015, 2019). White lines mark the Dead Sea Transform (DST) zone between the Western Marginal Fault (WMF), and the Eastern Marginal Fault (EMF). The sharp NNE-striking gravity gradient follows the WMF, which comprises the main DST strand and plate boundary between the Sinai sub-plate on the west and the Arabian plate on the east. Unlike the WMF, the EMF is not associated with a continuous and sub-parallel gravity gradient, although it constitutes a normal fault bordering the ~5 km deep Kinneret-Kinarot basin (KKB). Note the prominent gravity anomalies of the Yarmouk River. Thick black dashed ellipse marks the suggested extent of the Yarmouk Cover Basalt volcano. Black stars mark previously mapped volcanic centers. Israel Transverse Mercator (ITM) coordinates divided by 1,000. Abbreviations are similar to previous figures.

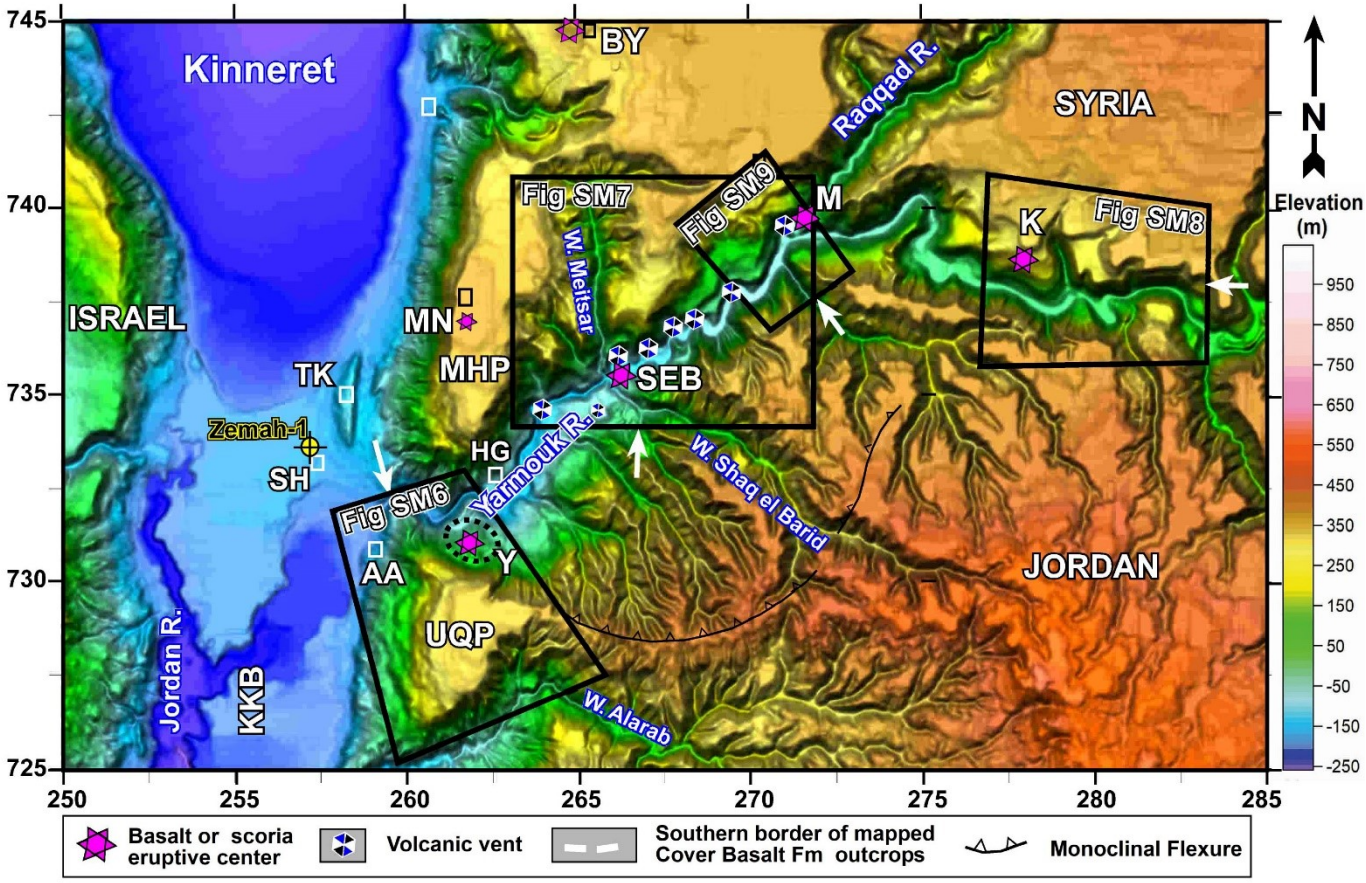

Figure SM5 – Elevation map showing the location of volcanic eruption centers and Zemah-1 well. Black frames mark the location of the following figures, including air photos and their view direction (marked by arrow). Note the concentric peripheral flexure south of the Yarmouk River gorge (Jordan) that centers around the Raqqad volcanics. Abbreviations are similar to previous figures. Israel Transverse Mercator (ITM) coordinates divided by 1,000.

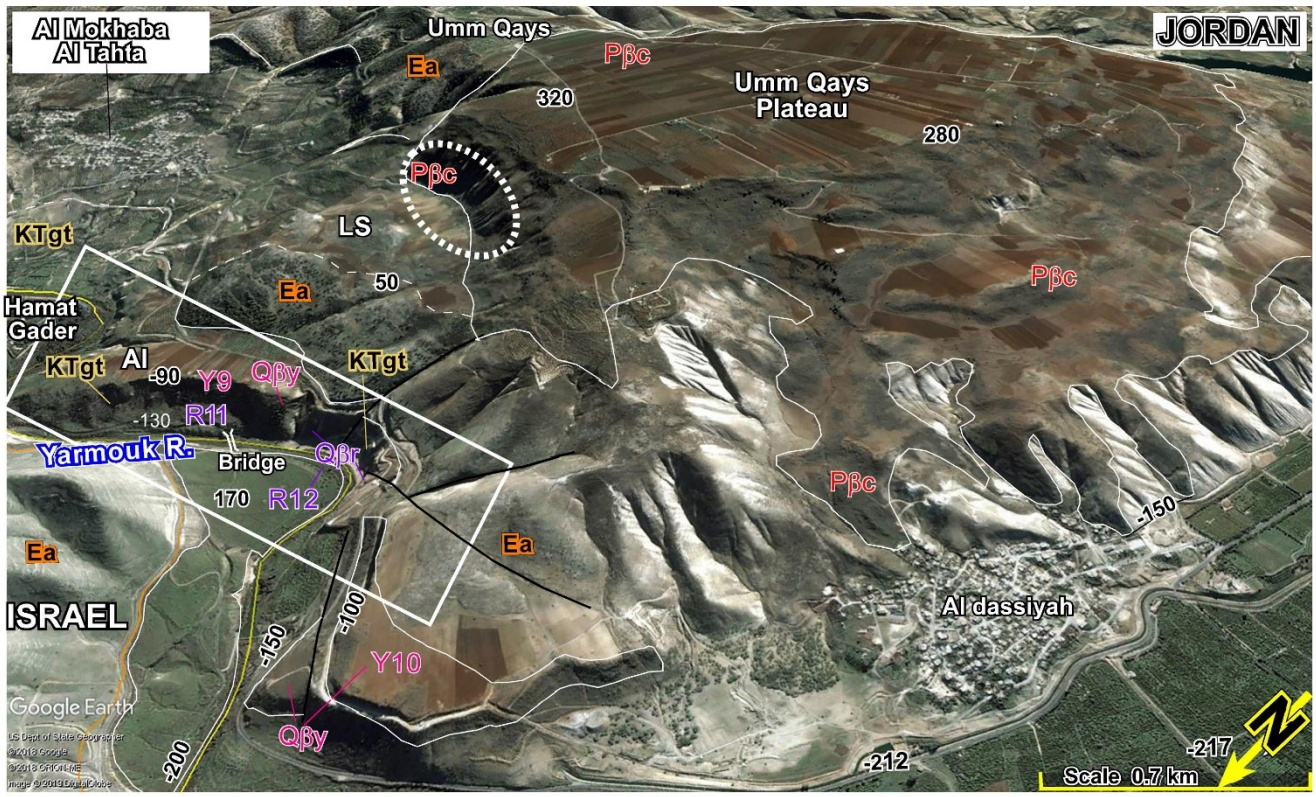

Figure SM6 – A southeastward facing Google Earth-based air-photo overlaid by geological contacts of Ghareb & Taqiye formations (KTgt; MCM in Jordan), Adulam Formation (Ea; URC in Jordan), the basalt units: Cover Basalt (Pβc), Yarmouk Basalt (Qβy) and Raqqad Basalt (Qβr) and landslides (LS) from Gilad toward the Yarmouk River. The yellow line marks the Jordan-Syria border along the Yarmouk River. Y9 – Y10 (magenta) Yarmouk Basalt terraces mark the westward downstream lava flows from the Koayiah Volcano; R11, R12 (purple) Raqqad Basalt terraces mark the westward downstream lava flows from the Shaq el Barid Volcano. This air photo emphasizes the westward basalt flows from the Umm Qays Plateau (~300 m high a.s.l) to Al Adassiyah (~ -150 m b.s.l). The white dash ellipse marks the southern relict of the Cover Basalt volcano termed Yarmouk Volcano. The white frame delimits terraces relicts that are better shown by Fig. 12B.

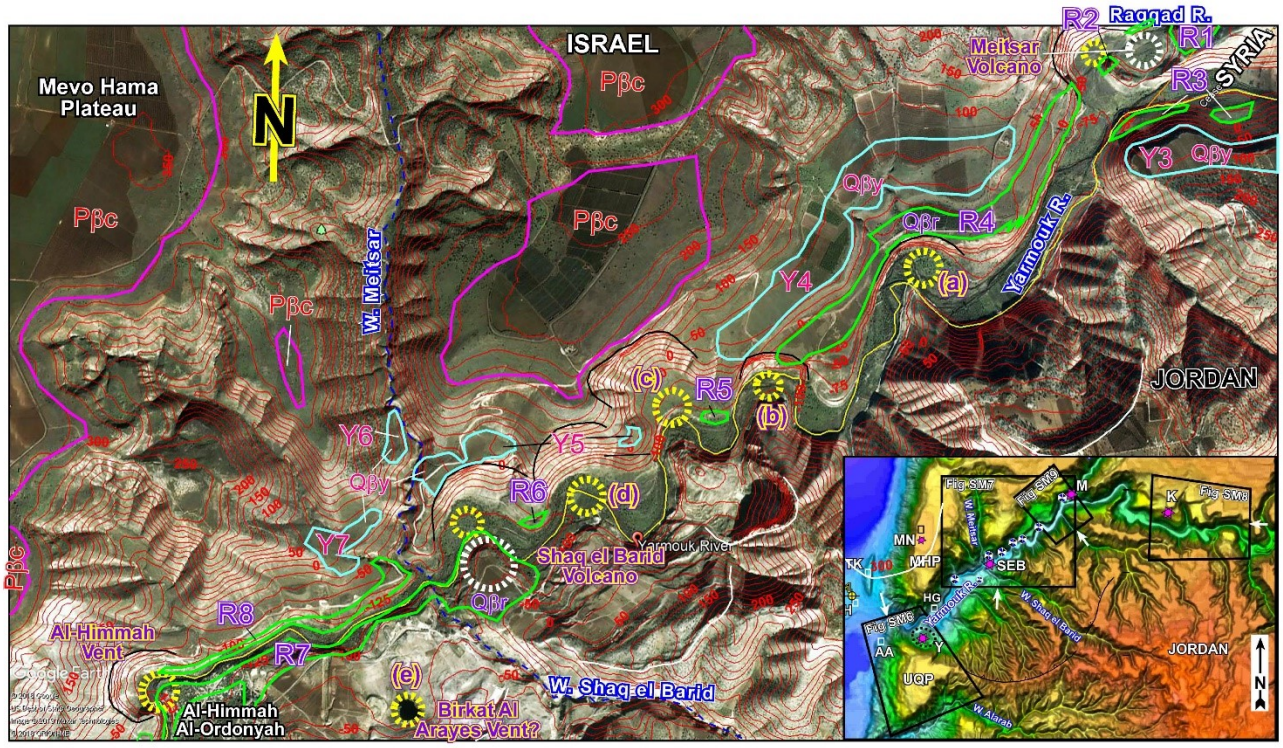

Figure SM7 – A northward facing Google Earth-based air-photo overlaid by geological contacts of basalt units, and DTM-based red topographic contours; location and viewpoint appear in the inset and Fig. SM5. White lines on the southern riverbank mark crescentic landslide scars. Black lines on the northern riverbank indicate incomplete steep sidewalls of covered volcanic vents, similar to Al-Himma Vent. Postulated vents are marked as (a)-(d), along the concealed Yarmouk fault. These vents diverted the Yarmouk River into its meanders.

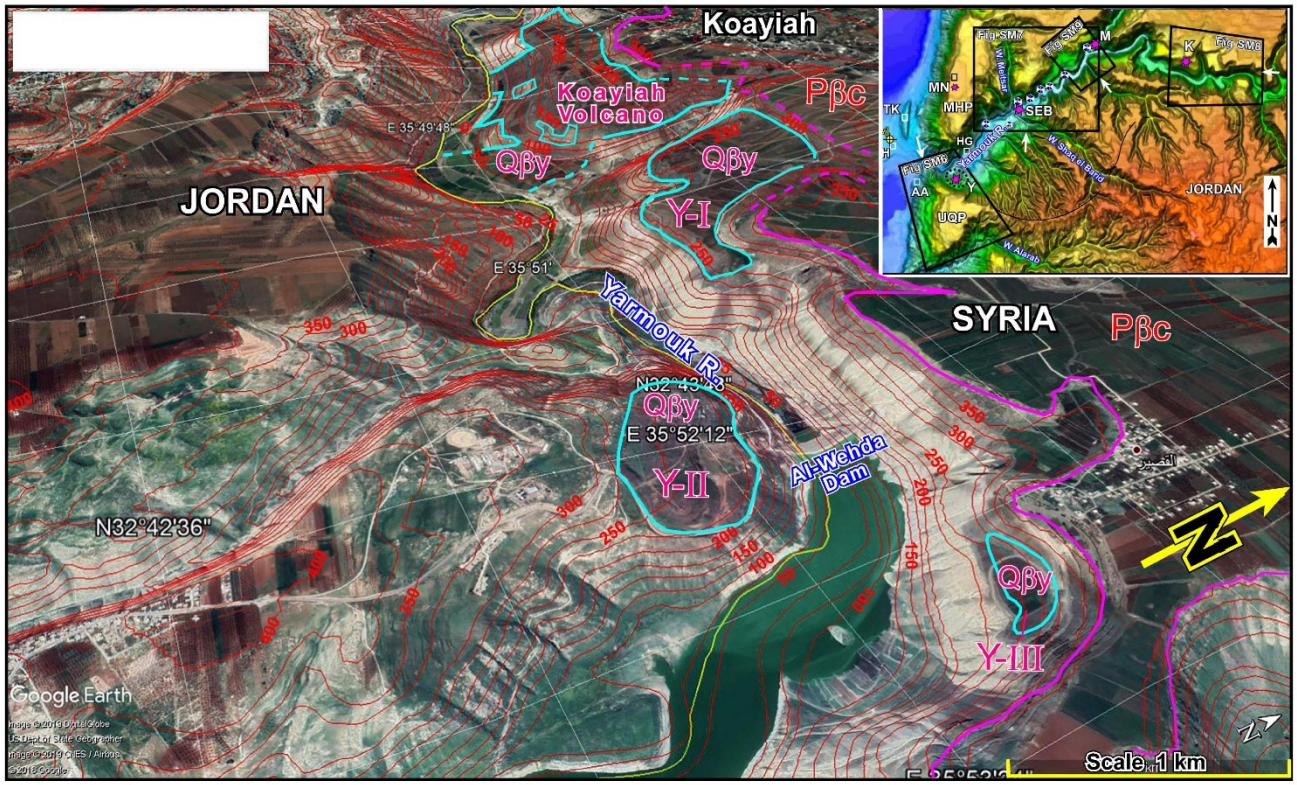

*Figure SM*8 – A westward-facing Google Earth-based air-photo overlaid by Digital Terrain Model (DTM) - based red topographic contours, and geological contacts of basalt units: Yarmouk Basalt (Qβy) - pale blue; Cover Basalt (Pβc), magenta. The yellow line marks the Jordan-Syria border along the Yarmouk River. Y-I – Y-III Yarmouk Basalt terraces mark the northeastward most upstream lava flows from the Koayiah Volcano.

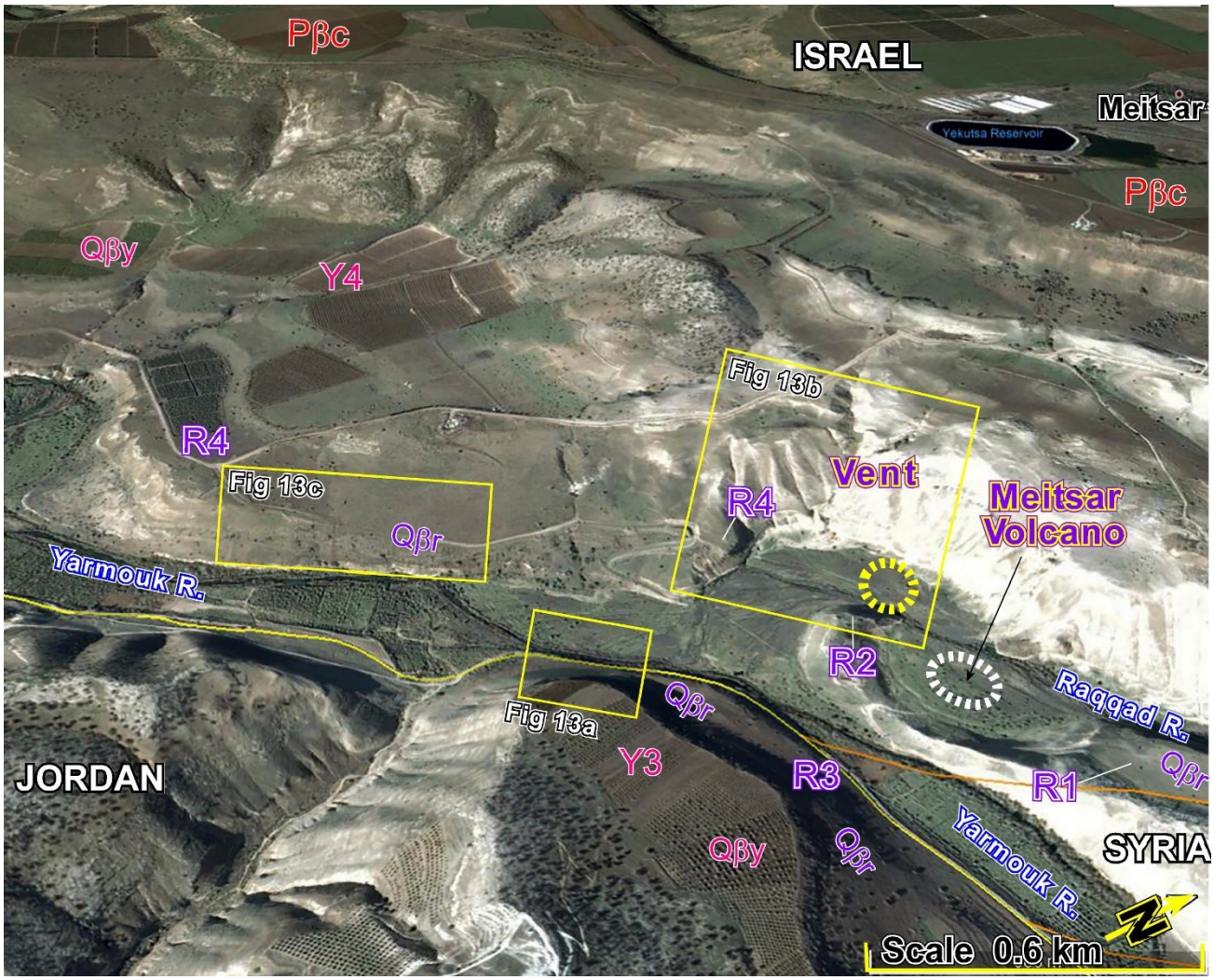

Figure SM9 – Air-photograph (modified after Google Earth) view toward the west where the Yarmouk and the Raqqad Basalt form terraces in different heights. Note the cirque of the Meitsar basalt volcano (black dashed line) and vent (yellow dashed line) cut by the Raqqad River. The yellow frames mark the location of the field photographs (Fig. 13 in the main text).

Figure SM10 – Photograph of the Shak El Barid railway bridge on the Yarmouk River, view toward the south on R7 basalt terrace (Fig. 14). The ability to see this outcrop on the non-accessible border between Israel and Jordan allows us to assume a similar situation in the close by (~300 m) Shak El Barid basaltic cone. The Raqqad basalt, which is ~25 m thick, starts from the river channel.

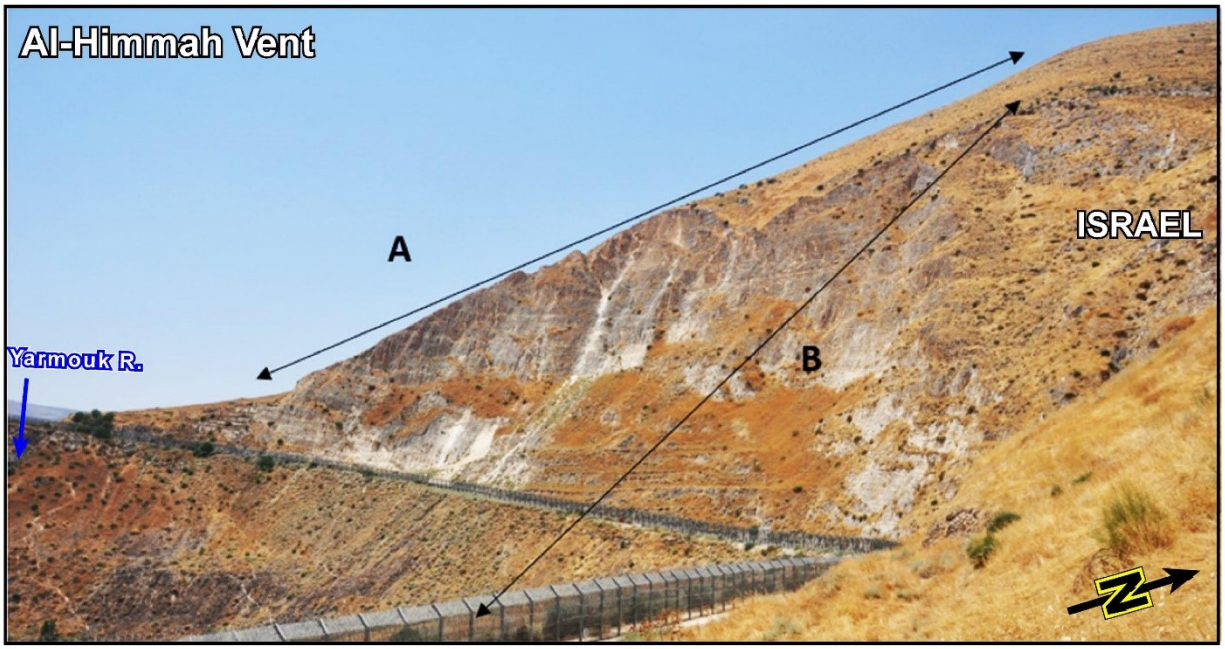

Figure SM11 – Photograph of the sidewalls of the Raqqad Basalt Volcanic vent Al-Himma (Fig. 14). Note the gradient difference between the typical moderate Yarmouk riverbank slope (A) and the steep sidewall of the vent (B).

Figure SM12 – Photograph, Birkat Al Arayes, Jordan, ~200m in diameter pond in a low depression (20-60 m) within landslide, south of the Yarmouk River (Fig. 14). The unusual occurrence, closeness to other volcanic vents and similarity to crater lakes brought us to speculate that it is a crater lake.

References

BEHAR, N., SHAAR, R., TAUXE, L., ASEFAW, H., EBERT, Y., HEIMANN, A., KOPPERS, A. A. & RON, H. 2019. Paleomagnetism and paleosecular variations from the Plio-Pleistocene Golan Heights volcanic plateau, Israel. Geochemistry, Geophysics, Geosystems 20(9), 4319-35.

DAVIS, M., MATMON, A., FINK, D., RON, H. & NIEDERMANN, S. 2011. Dating Pliocene lacustrine sediments in the central Jordan Valley, Israel – Implications for cosmogenic burial dating. Earth Planet. Sci. Lett., 305 (3 - 4), 317 - 327, DOI: 10.1016/j.epsl.2011.03.003. Michelson & Mor, 1987

GRADSTEIN, F. & OGG, J. 2004. Geologic time scale 2004–why, how, and where next! Lethaia 37(2), 175-81.

HEIMANN, A. & BRAUN, D. 2000. Quaternary stratigraphy of the Kinnarot Basin, Dead Sea Transform, northeastern Israel. Israel Journal of Earth Sciences 49.

HEIMANN, A. 1990. The development of the Dead Sea Rift and its margins in northern Israel during the Pliocene and the Pleistocene. p. 83 (in Hebrew; English summary). Jerusalem: Geological Survey of Israel.

HEIMANN, A., STEINITZ, G., MOR, D. & SHALIV, G. 1996. The Cover Basalt Formation, its age, and its regional and tectonic setting: Implication from K-Ar and 40Ar/39Ar geochronology. Israel Journal of Earth Science 45, 55-71.

INBAR, M. & GILICHINSKY, M. 2009. New Ar-Ar dates from lava flows and cinder cones in the Golan Heights—some geomorphic implications. Isr Geol Soc Meet, Kfar Blum, Israel.

MARCUS, E. & SLAGER, J. 1985. The sedimentary-magmatic sequence of the Zemah 1 Well (Jordan Dead Sea Rift, Israel) and its emplacement in time and place. Israel Journal of Earth Science 34, 1-10.

MARTINEZ-NAVARRO, B., BELMAKER, M. & BAR-YOSEF, O. 2009. The large carnivores from 'Ubeidiya (early Pleistocene, Israel): biochronological and biogeographical implications. Journal of Human Evolution 56(5), 514-24.

MOR. D. & STEINITZ. G., 1985. The History of the Yarmouk River based on K-Ar dating and its implication of the development of the Jordan Rift. Isr. Geol. Surv. Rep. GS1/40/85, 18 p.

ROSENTHAL, M., BEN-AVRAHAM, Z. & SCHATTNER, U. 2019. Almost a sharp cut–A case study of the cross point between a continental transform and a rift, based on 3D gravity modeling. Tectonophysics 761, 46-64.

ROSENTHAL, M., SEGEV, A., RYBAKOV, M., LYAKHOVSKY, V. & BEN-AVRAHAM, Z. 2015. The deep structure and density distribution of northern Israel and its surroundings. Rep GSI/12/2015, Geological Survey of Israel, Jerusalem.

ROZENBAUM, A. G., SANDLER, A., ZILBERMAN, E., STEIN, M., JICHA, B. R. & SINGER, B. S. 2016. 40Ar/39Ar chronostratigraphy of late Miocene−early Pliocene continental aquatic basins in SE Galilee, Israel. Geological Society of America Bulletin 128, 1383-402.

SANDLER, A., NATHAN, Y., ESHET, Y. & RAAB, M. 2001. Diagenesis of trioctahedral clays in a Miocene to Pleistocene sedimentary-magmatic sequence in the Dead Sea Rift, Israel. *Clay Minerals* 36(1), 29-47.

SCHATTNER, U., SEGEV, A., MIKHAILOV, V., RYBAKOV, M. & LYAKHOVSKY, V. 2019. Magnetic Signature of the Kinneret–Kinarot Tectonic Basin Along the Dead Sea Transform, Northern Israel. Pure and Applied Geophysics, 1-17.

SEGEV, A. 2000. Synchronous magmatic cycles during the fragmentation of Gondwana: radiometric ages from the Levant and other provinces. Tectonophysics 325(3-4), 257-77.

SEGEV, A. 2017. Zemah-1, a unique deep oil well on the Dead Sea fault zone, northern Israel: A new stratigraphic amendment. Geol. Surv. Isr. Rep., GSI/21/2017, 26 p.

SHALIV, G. 1991. Stages in the tectonic and volcanic history of the Neogene basin in the Lower Galilee and the valleys. pp. 1-94. Jerusalem: Geological Survey of Israel.

STEIN, M. 2014. The evolution of Neogene-Quaternary water-bodies in the Dead Sea rift valley. In Dead Sea Transform fault system: reviews pp. 279-316. Springer.

STEINITZ, G. & LANG, B. 1984a. K-Ar results. Appendix 3 In: Marcus et al. (1984) Zemah 1, geological completion report. Oil Explor. (Investments) Ltd., Rep. 84/11, 47-54.

STEINITZ, G. & LANG, B. 1984b. K-Ar systematics of the 2674 m gabbro from Zemah 1 well. Program and abstracts. Isr. Geol. Soc., Annu. Meet. Arad, p. 97.

TCHERNOV, E. 1987. The age of the Ubeidiya Formation, an Early Pleistocene hominid site in the Jordan Valley, Israel. Israel Journal of Earth-Sciences 36(1-2), 3-30.

WEINSTEIN, Y., WEINBERGER, R. & CALVERT, A. 2013. High-resolution 40Ar/39Ar study of Mount Avital, northern Golan: reconstructing the interaction between volcanism and a drainage system and their impact on eruptive styles. Bulletin of Volcanology 75(5), 712.